Research Square

Preprints are preliminary reports that have not undergone peer review.
They should not be considered conclusive, used to inform clinical practice,
or referenced by the media as validated information.

# Investigation of Cyclo-Z Therapeutic Effect on Insulin Pathway in Alzheimer's Rat Model: Biochemical and Electrophysiological Parameters

**Alev Duygu Acun** ( duyguacun@akdeniz.edu.tr )
Akdeniz University https://orcid.org/0000-0003-1240-6342
**Deniz Kantar**
Akdeniz University: Akdeniz Universitesi
**Hakan Er**
Akdeniz University: Akdeniz Universitesi
**Orhan Erkan**
Akdeniz University: Akdeniz Universitesi
**Narin Derin**
Akdeniz University: Akdeniz Universitesi
**Piraye Yargıcoglu**
Akdeniz University: Akdeniz Universitesi

**Research Article**

**Keywords:** Amyloid-beta oligomer, insulin, Cyclo-Z, memory, EEG

**Posted Date:** July 1st, 2022

**DOI:** https://doi.org/10.21203/rs.3.rs-1741637/v1

**License:** This work is licensed under a Creative Commons Attribution 4.0 International License.
Read Full License

## Abstract

# Background

Cyclo (his-pro-CHP) plus zinc ($Zn^{+2}$) (Cyclo-Z) is the only chemical agent known to stimulate IDE synthesis and reduction of inactive cellular insulin fragments.

# Objectives

The aim of this study was to characterize the effects of Cyclo-Z on insulin pathway, memory functions and brain oscillations in the Alzheimer's disease (AD) rat model.

# Methods

The rat model of AD was established by bilateral injection of Aβ42 oligomer (2,5nmol/10µl) into the lateral ventricles. Cyclo-Z (10mg $Zn^{+2}$/kg and 0,2mg CHP/kg, daily) was administered orally by gavage for 21 days. At the end of the experimental period, memory tests and electrophysiological recordings were performed which followed by the biochemical analysis.

# Results

Aβ42 oligomers led to a significant increase in fasting blood glucose, serum insülin, Homeostatic Model Assessment for Insulin Resistance(HOMA-IR) and phospho-tau-Ser356 levels. Moreover, Aβ42 oligomers caused a significant decrement in body weight, hippocampal insulin, brain insulin receptor substrate(IRS-Ser612), and glycogen synthase kinase-3 beta(GSK-3β) levels. Also, Aβ42 oligomers resulted in a significant reduction in memory. The Cyclo-Z treatment prevented the observed alterations in the ADZ group except for phospho-tau levels and attenuated the increased Aβ42 oligomers levels in the ADZ group. We also found that the Aβ42 oligomer decreased the left temporal spindle and delta power during ketamine anesthesia. Cyclo-Z treatment reversed the Aβ42 oligomer-related alterations in the left temporal spindle power.

# Conclusions

Cyclo-Z prevents Aβ oligomer-induced changes in the insulin pathway, amyloid toxicity, and may contribute to the improvement of memory deficits and neural network dynamics in this rat model.

## Introduction

Alzheimer's Disease (AD) is a type of progressive dementia due to the accumulation of extracellular Aβ peptides and intracellular neurofibrillary tangles (NFT) [1]. To date, studies on AD have indicated that Aβ accumulation is the major factor in the pathogenesis of the disease. Oligomeric types of Aβ peptide are thought to trigger synaptic dysfunction, neurodegeneration and ultimately dementia [2–5]. The cellular pathology leading to neural network dysfunction has not been fully explained yet. However, it has been shown that Aβ exposure induces changes in presynaptic and postsynaptic synapses, while tau accumulations lead to synaptic conduction disorder and disrupt neural synaptic network dynamics [6, 7].

In recent studies, it has been emphasized that brain insulin resistance is an early feature of AD and develops before the onset of AD symptoms. Increasing insulin resistance contributes to cognitive impairment both before and after AD-specific molecular changes [8]. It is known that insulin has an important role in the regulation of energy metabolism and neuronal vitality in neurons and acts as a growth factor in the brain. The insulin signaling mechanism in the brain is essential for the formation of synaptic plasticity that plays a central role in cognitive functions [9]. Aβ oligomers (AβOs) are potent synaptotoxins that accumulate and act as synapse-specific ligands [10–12]. Insulin and Aβ are both amyloidogenic peptides that share a common sequence recognition motif. Therefore, AβOs can bind to the insulin receptor and inhibit its autophosphorylation [13]. They also trigger the detachment of the insulin receptor from the plasma membrane, resulting in decreased surface insulin receptors and insulin sensitivity [14, 15]. When amyloid-β oligomers bind to insulin receptors, they block the downstream pathway of insulin signaling. This results in NFT formation with overproduction of Aβ due to tau hyperphosphorylation and excessive γ-secretase activation [16]. Insulin signal also provides a physiological defense mechanism against synapse loss caused by oligomers [15, 17].

When the insulin binds to its receptor, it activates the phosphatidylinositol-3 kinase (PI3K) → Protein kinase B (PKB/Akt) pathway by phosphorylating the adapter proteins such as IRS-1 and 2. Activation of this pathway phosphorylates GSK-3β and inactivates it [9]. The insulin receptor acquires an intrinsic tyrosine (Thr) kinase activity when activated by insulin. Tyrosine kinase activity triggered by insulin binding downregulates the oligomer binding sites in neurons [15, 17]. Thus, insulin signalling protects from the long-term potentiation (LTP) disorder caused by oligomers and the accumulation of hyperphosphorylated tau [18]. Moreover, observed increment of brain insulin resistance causes a decrement in the degradation of Aβ oligomer by reducing insulin-degrading enzyme (IDE) and Neprilysin (NEP) levels in AD. This leads to worsening insulin resistance and the production of more toxic AβOs [19–21]. Therefore, potentiation of insulin signaling and Aβ oligomer degradation in AD seem to be an important therapeutic target.

Zinc has been shown to give insulin-like effects by facilitating insulin signaling [22]. Also, $Zn^{+2}$ stimulates both IDE and NEP synthesis which are known to cleave Aβ peptides [23]. Besides, $Zn^{+2}$ deficiency is a common condition in AD [24, 25]. Thus, $Zn^{+2}$ dyshomeostasis may play a critical role in the pathogenesis of AD, and $Zn^{+2}$ chelation is a potential therapeutic approach [26]. $Zn^{+2}$ deficiency is mostly caused by impaired intestinal $Zn^{+2}$ absorption and $Zn^{+2}$ uptake into the cell. The normal

elemental $Zn^{+2}$ absorption mechanism takes place through facilitated diffusion, through Zn transporter (ZnT) proteins. These ZnTs contain a large number of histidines similar to histidyl-proline diketopiperazine (cyclo [His-Pro]; CHP). CHP is a cyclic form of the amino acids L-histidine and proline. Histidine-proline-rich glycoproteins play an important role in $Zn^{+2}$ transport [27]. Since CHP contains a L-histidine molecule, it has the ability to chelate $Zn^{+2}$ and stimulate intestinal $Zn^{+2}$ absorption and $Zn^{+2}$ uptake [28]. This cyclic form helps $Zn^{+2}$ transport independent of the normal elemental $Zn^{+2}$ transport system [29]. Studies have shown that it is not very effective when CHP or $Zn^{+2}$ has applied alone [1]. The therapeutic effectiveness increases when they are applied together as Cyclo-Z, the combination of CHP and $Zn^{+2}$.

It is not entirely known how the altered insülin pathway plays a role in the early stage of AD. At the same time, the molecular pathways associated with the hyperphosphorylation of the tau protein due to the altered insulin signaling have still not been clearly elucidated. In this study, we demonstrated the molecular changes in the insulin signaling pathway observed in the Aβ oligomers-induced early AD rat model. We examined the effects of changes in the insulin signaling pathway on tau phosphorylation, Aβ accumulation, cognitive functions, and brain oscillations. Besides, Cyclo-Z has been suggested as a potential stimulator agent for insulin signaling. So, we examined how altered insulin signaling due to the Cyclo-Z agent affects AβOs induced neuropathology, cognitive functions, and brain oscillations.

## Materials And Methods

# Animals and treatment

The rats were obtained from Akdeniz University Animal Care Unit. Male albino Wistar rats aged 3 months, weighing 250–300 g were housed in stainless steel cages in groups of 4 rats per cage and given food and water ad libitum. The body weights of the animals were recorded twice, at the beginning of the surgical procedure and before the sacrifice of the animals. Animals were fasted 12 hours before fasting blood glucose was measured. Animals were maintained at 12 h light-dark cycles and a constant temperature of 23 ± 1°C at all times. Animals were divided into four groups (n = 15 each group): (1) sham-operated (1,25 µl DMSO + 8,75 µl PBS/10µl) intracerebroventricularly (i.c.v) injection plus water treatment (SH); (2) sham-operated (1,25 µl DMSO + 8,75 µl PBS/10µl) i.c.v. injection plus Cyclo-Z treatment (10 mg Zn/kg and 0,2 mg SHP/kg gavage) (SHZ); (3) Aβ42 oligomer (2,5 nmol/10 µl) i.c.v. injection plus physiological water treatment (AD); (4) Aβ42 oligomer (2,5 nmol/10 µl) i.c.v. injection plus Cyclo-Z treatment (10 mg Zn/kg and 0,2 mg SHP/kg gavage) (ADZ). Drugs were administered seven days after the surgical procedure. Treatment occurred once a day for 21 days. Zinc chloride was purchased from Molar Kimya (MZK.100310.1000). The purity of Zinc chloride was > 98%. Cyclo was purchased from Santa Cruz (Santa Cruz Biotechnology, Europe). Cyclo has a molecular formula of $C_{11}H_{14}N_4O_2$ and a molecular weight of 234,26 g/mol. 50 mg of Cyclo and 2.5 g $Zn^{+2}$ were dissolved in 1 L water. The dosage was chosen according to the results of an earlier study [30]. Aβ1–42 oligomers were prepared in accordance with the literatüre [31]. Aβ1–42 (Sigma-Aldrich, USA, product no: A9810) peptides were

dissolved in DMSO to a concentration of 2 mmol and then diluted 8 times in sterile PBS, vortexed for 30 minutes at room temperature, then centrifuged at 15000×g at 4°C for 1 hour. Supernatants (250 µl) were aliquoted (25 µl) and frozen at -20°C. Aβ-42 oligomers were used within 24 hours when heated to 4°C. Since DMSO is a toxic substance, 10 µl solution prepared with 1.25 µl DMSO and 8.75 µl PBS was given to the sham groups.

# Animal preparation

The rat model of AD was established as described previously [32, 33]. Rats were anesthetized with a combination of ketamine (80 mg/kg, i.p.) and xylazine (5 mg/kg, i.p.) and then placed in a standard stereotaxic apparatus. A middle sagittal incision was made in the scalp and was sterilized using standard procedures. Bilateral holes were drilled in the skull using a dental drill over the lateral ventricles (AP: −0.8 mm, ML:±1.4 mm, DV: −4.0 mm). Rats in AD and ADZ groups were injected with 2,5 nmol/10 µl Aβ-42 oligomers at a rate of 0.5 µl/min. The syringe was removed 5 min after the injection. The SH and SHZ groups received 10µl solution prepared with 1.25 µl of DMSO and 8.75 µl of PBS. After surgery, the scalp was sutured, and sulfamethoxazole was sprinkled on the wound to prevent infection. For measurement of fasting blood glucose levels, the tail region was bled and then measured by the glucose oxidation method using a glucometer (plusMED Blood GlucoseMeter, Accuro, pM1-300, Bionime Corporation, Taiwan). In addition, penicillin (40,000 U) was injected intramuscularly into the gluteus, once a day for 3 days. It waited for one week for them to heal and for the Aβ-42 oligomers to form the pathological damage. After the rats recovered, gavage and learning experiments were started. At the end of the gavage application, learning experiments were performed and then electrode implantation was performed for electrophysiological recordings.

# Surgery protocols

Rats were anesthetized with a combination of ketamine (80 mg/kg, i.p.) and xylazine (5 mg/kg, i.p.) and then placed in a standard stereotaxic apparatus. For measurement of fasting blood glucose levels, the tail region was bled and then measured by the glucose oxidation method using a glucometer (plusMED Blood GlucoseMeter, Accuro, pM1-300, Bionime Corporation, Taiwan). During the anesthesia, the skull of the rats was placed in the stereotaxic apparatus and drilled for the implantation of electrodes. Stainless steel screw electrodes were implanted bilaterally over the frontal (AP: 4.5 mm, ML: +2 and − 2 mm, DV: +1.8 mm), temporal (AP: -8.0 mm, ML: +6.6 and − 6.6 mm, DV: 3.3 mm), the reference and ground electrodes were inserted into the cerebellum (AP: -12.72 mm, ML: 2.5 and − 2.5 mm, DV: 3.2 mm). After the electrodes were placed, the rats were removed from the stereotaxic device and electrophysiological recordings were taken.

# Biochemical and western blot investigations

Immediately after taking the electrophysiological recordings, blood was drawn from the vein of the rats into EDTA tubes under ketamine-xylazine anesthesia. Afterward, the brain tissues were purified from the

blood by cardiac perfusion using isotonic with heparin through the cardiac cannula. The excised brain tissues were frozen in liquid nitrogen and stored at -80°C for measurements of biochemical parameters.

# Measurement of Insulin Amount in Plasma and Hippocampus Tissue Homogenates

Insulin levels in the supernatants of plasma and hippocampus tissue homogenates were measured using a commercially available ELISA kit (Bioassay Technology Laboratory, E0707Ra) in accordance with the manufacturer's instructions. These kits contain 96 well plates coated with rat insulin antibody. Biotinylated rat insulin antibody is then added and binds to the insulin in the sample. Insulin-specific horseradish peroxidase (HRP) conjugate polyclonal antibody is added. Thus, the immobilization of insulin is ensured and a sandwich model is created. Therefore, streptavidin-HRP is then added and binds to the Biotinylated insulin antibody. After incubation, unbound Streptavidin-HRP is washed 5 times during the wash step. After incubation and washing, unbound components are removed. The substrate solution is then added. When the substrate solution is added, the HRP reacts with the enzyme, leading to color formation. In this method, color formation is observed only in the wells containing insulin. Color develops in proportion to the amount of insulin in the rat. The reaction is terminated by adding an acidic stop solution. Optical density (OD) is measured spectrophotometrically at 450 nm. The sample amount of insulin is calculated with a standard curve plot. Peripheral insulin resistance was assessed using the HOMA-IR formula (fasting insulin (mIU/l) x fasting blood glucose (mM)/22,5) (Yang, Chen et al. 2017).

# Measurement of Aβ1–42 Oligomer Amount in Total Brain and Hippocampus Tissue Homogenates

Aβ1–42 oligomer levels in the supernatants of total brain and hippocampus tissue homogenates were measured using a commercially available ELISA kit (YL biont-YLA0372RA) in accordance with the manufacturer's instructions. Aβ1–42 is added to wells pre-coated with Aβ1–42 monoclonal antibody and then incubated. After that, biotin-labeled anti-Aβ1–42 antibodies were added to combine with streptavidin-HRP. After incubation and washing, unbound components are removed. Substrate solutions A and B are then added. When the substrate solution is added, the HRP reacts with the enzyme, leading to color formation. In this method, color formation is observed only in wells containing Aβ1–42. Color develops in proportion to the amount of rat Aβ1–42. The reaction is terminated by adding an acidic stop solution. The OD is measured spectrophotometrically at 450 nm. The amount of sample Aβ1–42 is calculated by the standard curve plot.

# Measuring Protein Levels with the Western Blot Technique

For the preparation of tissue homogenates, frozen brain samples were crushed with liquid nitrogen, and then the crushed brain tissue samples were suspended in lysis buffer (50mM Tris–HCl, pH 7,4, 100 µM EDTA, 100 µM EGTA, 1% NP-40, 0.1% SDS, 0.1% deoxycholic acid) to which protease inhibitor cocktail tablets were added. The protein concentrations of supernatants after centrifugation (10,000g, 10 min, at 4 C) were measured with the BCA assay kit (Pierce) according to the manufacturer's instructions. After the

protein content was determined, equal amounts of proteins (20µg/ml) were loaded into each well and separated by 12% SDS polyacrylamide gel electrophoresis at 100V 30 mA for approximately 1,5 hours. Proteins separated by gel electrophoresis were transferred to the polyvinylidene difluoride membrane with a transfer system (Trans-Blot Turbo BioRad) at 25V 1.3mA for 10 minutes. After this step, the membranes were taken in TTBS (0.1% Tween-20, 10 mM Tris and 150 mM NaCl solution (containing 3% albumin)) and incubated for 1 hour at room temperature. After the incubation phase, primary antibodies were prepared in TTBS solution containing 3% albumin according to the desired protocol and incubated overnight (+ 4$^{o}$C). These primary antibodies are IDE (Ylbiont, YID2780), NEP (SinoGeneClon Biotech Co., SG-0527-R), p-IRS1 (Ylbiont, YIG0585), p-GSK-3β (SinoGeneClon Biotech Co., SG-5368R), p-Tau (ser356) (ThermoFisher, 44-752G). The membranes were then washed with TTBS solution 3 times for 10 minutes, and then the secondary antibody (Goat anti-rabbit IgG/HRP-Ylbiont, YIF0010) step, which was suitable for the primary antibodies, was started. Finally, bound antibodies were detected with the chemiluminescence-based HPR Substrate System. Membranes were exposed to Hyperfilm. The results obtained were analyzed using Image J software and protein expression was determined relative to the proportion of GAPDH target protein conjugated.

# Behavioral Testing

The novel object recognition memory and object location memory tests were modified from Roozendaal et al., adapted to rats [34]. The system in which the experiment was carried out consists of a box measuring 40 cm x 40 cm x 40 cm, evenly illuminated, with a white matte base and sides. The experiment was carried out in a soundproofed room to prevent any external stimulus from interfering with the experimental parameters during the experiment. Object location test was performed for each rat 3 days after the new object recognition test.

# Novel Object Recognition Test

The novel object recognition test consists of two phases: the training phase and the testing phase. During the training phase, two identical objects (A1-A2) were placed in the experimental system at two opposite positions at the same distance from the nearest corner. The rats were then released from the center to the field and allowed 5 minutes to explore these two identical objects (A1-A2). The rats that completed the training phase were taken to the test phase 24 hours after they were placed back in their cages. In order to test the novel object recognition memory during the test phase, a copy of the familiar object (A3) and a new object (B1) were placed in the same place as during the training experiment. Each of the objects used in the experiment was fixed to the floor to prevent its movement. The behavior of the rats during the training and testing phases was recorded with a video camera and used to determine the time the rats spent with the objects. To preclude the existence of olfactory cues, the entire box and objects were always thoroughly cleaned with 70% ethanol after each trial. In the novel object recognition test, discrimination index (%) values showing memory strength were analyzed. The discrimination index was calculated by multiplying the difference between the time to examine the new and the old object divided by the total time spent examining both objects by 100.

# Object Location Test

Object location testing consists of two phases: the training phase and the testing phase. During the object location test training phase, two identical objects (A1-A2) were placed in the experimental system. The rats were then released from the center to the field and allowed 5 minutes to explore these two identical objects (A1-A2). The rats that completed the training phase were taken to the test phase 24 hours after they were placed back in their cages. To test the object location memory in the test phase, a copy of the familiar object (A3) was placed in its place in the training phase, while the other familiar object (A4) was placed in a different location from the training phase. Each of the objects used in the experiment was fixed to the floor to prevent its movement. The behavior of the rats during the training and testing phases was recorded with a video camera and used to determine the time the rats spent with the objects. To preclude the existence of olfactory cues, the entire box and objects were always thoroughly cleaned with 70% ethanol after each trial. The discrimination index (%) values were analyzed in the object location test. The discrimination index (%) is an equation obtained by dividing the difference of the time spent on the changed object from the time spent on the object in the old location by the total time and multiplying by 100.

# Recordings and analysis of EEG

All recordings were taken in a sound-attenuated, electromagnetically shielded recording room. Spontaneous EEG recordings were taken for 10 minutes from rats under ketamine-xylazine anesthesia through screw electrodes made of stainless steel. The EEG was recorded bilaterally from frontal (AP: 4,5 mm, ML: +2 and − 2 mm, DV: +1,8 mm) and temporal (AP: -8,0 mm, ML: +6,6 and − 6,6 mm, DV: 3,3 mm) locations. All electrode impedances were < 5 kOhm. The EEG signal was amplified (Brainamp EEG/EP Amplifier, Brain Products, Munich, Germany), band-pass–filtered (0,1–500 Hz), and digitized at a 1000 Hz sampling rate (BrainVision Recorder, Brain Products, Munich, Germany). EEG analysis was conducted offline. All EEG analyzes were performed using the program Brain Vision Analyzer 2.2 (Brain Products GmbH; Gilching, Germany). First, 0,1–150 Hz and 50 Hz Notch filters were applied to the EEG data, and then it was divided into 10-second windows. Frequency analysis was performed using a fast Fourier transform (FFT) algorithm with Hanning window with 10% taper length using the BrainVision Analyzer software (BrainProducts GmBH, Munchen). Spectral powers of each rat were averaged for each electrode location. The EEG variables chosen were absolute power in four frequency bands, delta (0,5–4 Hz), alpha/spindle (8–12 Hz), and beta (13–29 Hz).

# Statistical analysis

The statistical analyses of the obtained data were performed using SPSS 23.0 (SPSS, Chicago, IL, USA) software for Windows. Statistical comparisons between groups for object recognition and location tests, biochemical experiments, and western blot analysis were performed by using one-way ANOVA and post hoc Tukey test. Electrophysiological data were analyzed by means of a repeated measure ANOVA (rANOVA) including the between-subject factor groups and the within-subject factor electrode locations (Bonferroni post hoc test). Greenhouse–Geisser corrected p-values are reported. Weight changes were examined via rANOVA included between-subject factor groups and within-subject factor days. (Tukey post hoc test). Results are expressed as mean ± standard error. Significance levels were set at $P < 0.05$. All

experimenters were blinded to animal experimental group membership during data collection and analyses.

## Results

# Changes in body weight

The body weights of the animals were recorded twice, at the beginning of the surgical procedure and before the sacrifice of the animals. Body weight values of sham and experimental groups are given in Table 1. There was a significant difference between groups [$F(3,48) = 11.39$, $p < 0.001$]. The body weight gain of the animals was significantly decreased in the AD (20,38 ± 13,26 g) versus the SH (31,46 ± 2,17 g) ($p < 0.001$). Cyclo-Z treated ADZ (28,15 ± 2,93 g) group had higher body weight gain levels versus the AD group ($p < 0.001$). Although it was observed that the weight gain of the SHZ group was less than that of the SH group, Cyclo-Z treatment alone had no significant impact on body weight gain.

Table 1
Weight changes of sham and experimental group animals. n = 13 for each group.

| Groups | Body weight measurement 1 (g) | Body weight measurement 2 (g) | Weight gain (g) |
|---|---|---|---|
| **SH** | 239,31 ± 5,86 | 270.77 ± 8,40 | 31,46 ± 2,17 |
| **SHZ** | 275,00 ± 5,86 | 280,77 ± 8,40 | 5,77 ± 3,54 |
| **AD** | 308,62 ± 5,86 | 288,23 ± 8,40 | -20,38 ± 13,26*** |
| **ADZ** | 259,31 ± 5,86 | 287,46 ± 8,40 | 28,15 ± 2,93ξξξ |

*: Significant vs SH group, #: Significant vs SHZ group, ξ: Significant vs AD group. *: $p < 0.05$; **: $p < 0.01$; ***: $p < 0.001$, #: $p < 0.05$; ##: $p < 0.01$; ###: $p < 0.001$, ξ: $p < 0.05$, ξξ: $p < 0.01$, ξξξ: $p < 0.001$

# Plasma Fasting Blood Glucose Levels

Mean values of plasma fasting blood glucose levels are given in Fig. 1A. There was a statistically significant difference in plasma fasting blood glucose levels between groups [$F(3,20) = 24.88$, $p < 0.001$]. The plasma fasting blood glucose levels were significantly increased in the AD (191,33 ± 5,524 mg/dL) versus the SH (143,00 ± 6,033 mg/dL) ($p < 0.01$). ADZ (161,00 ± 5,092 mg/dL) group had lower plasma fasting blood glucose levels versus AD group ($p < 0.05$). The plasma fasting blood glucose levels were significantly increased in the SHZ (226,00 ± 10,957 mg/dL) versus the SH ($p < 0.001$).

# Serum Insulin Levels

Mean values of serum insülin levels are given in Fig. 1B. There was a statistically significant difference in serum insülin levels between groups [$F(3,28) = 7.84$, $p < 0.01$]. The serum insülin levels were significantly increased in the AD (2,71 ± 0,074 mIU/L) versus the SH (2,37±,0.059 mIU/L). The serum insülin levels

were significantly increased in the SHZ (2,69±,0.057 mIU/L) versus the SH ($p < 0.01$ for all comparisons). Although a slight decrease was seen in the serum insülin levels of the ADZ group vs the AD group. This decrement did not reach the significance level.

# Hippocampus Insulin Levels

Mean values of hippocampus insülin levels are given in Fig. 1C. There was a statistically significant difference in hippocampus insülin levels between groups [$F(3,20) = 3.64$, $p < 0.05$]. The hippocampus insülin levels were significantly decreased in the AD (0,162 ± 0,021 mIU/L) versus the SH (0,233 ± 0.016 mIU/L) ($p < 0.05$). Although a slight decrease was seen in the hippocampus insülin levels of the SHZ group vs the SH group. This decrement did not reach the significance level. Although a slight increase was seen in the hippocampus insülin levels of the ADZ group vs the AD group. This increment did not reach the significance level.

# HOMA-IR levels

Mean values of HOMA-IR levels are given in Fig. 1D. There was a statistically significant difference in HOMA-IR levels between groups [$F(3,20) = 9.21$, $p < 0.001$]. The HOMA-IR levels were significantly increased in the AD (1,276 ± 0,037) versus the SH (0,891 ± 0,046). The HOMA-IR levels were significantly increased in the SHZ (1,263 ± 0,095) versus the SH ($p < 0.01$ for all comparisons). Although a slight decrease was seen in the HOMA-IR levels of the ADZ group vs the AD group. This decrement did not reach the significance level.

# Total Brain AβO Levels

Mean values of total brain AβO levels are given in Fig. 1E. There was a statistically significant difference in total brain AβO levels between groups [$F(3,28) = 7.21$, $p < 0.01$]. The total brain AβO levels were significantly increased in the AD (15,90 ± 0,913 mg/protein) versus the SH (11,46 ± 0,573 mg/protein). The total brain AβO levels were significantly decreased in the ADZ (11,24 ± 1,154 mg/protein) versus the AD. The total brain AβO levels were significantly increased in the SHZ (14,91 ± 0,792 mg/protein) versus the SH ($p < 0.05$ for all comparisons).

# Hippocampus AβO Levels

Mean values of hippocampus AβO levels are given in Fig. 1F. There was a statistically significant difference in hippocampus AβO levels between groups [$F(3,28) = 21.41$, $p < 0.001$]. The hippocampus AβO levels were significantly increased in the AD (14,250 ± 0,817 mg/protein) versus the SH (7,920 ± 0,645 mg/protein) ($p < 0.001$). The hippocampus AβO levels were significantly decreased in the ADZ (8,380 ± 0,528 mg/protein) versus the AD ($p < 0.001$). The hippocampus AβO levels were significantly increased in the SHZ (10,369 ± 0,604 mg/protein) versus the SH ($p < 0.05$).

# Total Brain p-Tau (Ser356) Levels

Mean values of total brain p-Tau (Ser356) levels are given in Fig. 2A. There was a statistically significant difference in total brain p-Tau (Ser356) levels between groups [$F(3,20) = 10.09$, $p < 0.001$]. Although a

slight increase was seen in the total brain p-Tau (Ser356) levels of the AD group vs the SH group. This increment did not reach the significance level. No statistically significant difference was observed between the SH and SHZ groups. The total brain p-Tau (Ser356) levels were significantly increased in the ADZ (0,405 ± 0,075) versus the AD (0,705 ± 0,068) ($p < 0.05$). The total brain p-Tau (Ser356) levels were significantly increased in the ADZ (1,245 ± 0,075) versus the AD (1,015 ± 0.056) ($p < 0.01$). The total brain p-Tau (Ser356) levels were significantly increased in the ADZ versus the SH (0,833 ± 0,038) ($p < 0.001$) and SHZ (0,935 ± 0,041) ($p < 0.05$).

# Hippocampus p-Tau (Ser356) Levels

Mean values of hippocampus p-Tau (Ser356) levels are given in Fig. 2B. There was a statistically significant difference in hippocampus p-Tau (Ser356) levels between groups [$F(3,20) = 17.40$, $p < 0.001$]. The hippocampus p-Tau (Ser356) levels were significantly increased in the AD (0,516 ± 0,060) versus the SH (0,250 ± 0,042) ($p < 0.05$). The hippocampus p-Tau (Ser356) levels were significantly increased in the SHZ (0,466 ± 0,033) versus the SH ($p < 0.001$). The hippocampus p-Tau (Ser356) levels were significantly increased in the ADZ (0,866 ± 0,091) versus the AD ($p < 0.01$). The hippocampus p-Tau (Ser356) levels were significantly increased in the ADZ versus the SH and SHZ ($p < 0.001$).

# Total Brain p-IRS-1 (Ser612) Levels

Mean values of total brain p-IRS-1 (Ser612) levels are given in Fig. 2C. There was a statistically significant difference in total brain p-IRS-1 (Ser612) levels between groups [$F(3,20) = 6.91$, $p < 0.01$]. The total brain p-IRS-1 (Ser612) levels were significantly decreased in the AD (0,495 ± 0,023) versus the SH (0,686 ± 0.055) ($p < 0.05$). The total brain p-IRS-1 (Ser612) levels were significantly increased in the ADZ (0,693 ± 0,040) versus the AD ($p < 0.05$). Although a slight increase was seen in the total brain p-IRS-1 (Ser612) levels of the SHZ (0,777 ± 0.054) group vs the SH group. This increment did not reach the significance level. No statistically significant difference was observed between the ADZ and SHZ groups.

# Hippocampus p-IRS-1 (Ser612) Levels

Mean values of hippocampus p-IRS-1 (Ser612) levels are given in Fig. 2D. There was a statistically significant difference in hippocampus p-IRS-1 (Ser612) levels between groups [$F(3,24) = 16.42$, $p < 0.001$]. No statistically significant difference was observed between the AD and SH groups. The hippocampus p-IRS-1 (Ser612) levels were significantly increased in the SHZ (0.755 ± 0,042) versus the SH (0,508 ± 0,020) ($p < 0.001$). The hippocampus p-IRS-1 (Ser612) levels were significantly decreased in the AD (0,428 ± 0,043) versus the ADZ (0,644 ± 0,031) ($p < 0.01$). No statistically significant difference was observed between the ADZ and SHZ groups.

# Total Brain p-GSK-3β (Ser-21) Levels

Mean values of total brain p-GSK-3β (Ser-21) levels are given in Fig. 2E. There was a statistically significant difference in total brain p-GSK-3β (Ser-21) levels between groups [$F(3,24) = 8.31$, $p < 0.01$]. The total brain p-GSK-3β (Ser-21) levels were significantly decreased in the AD (0,405 ± 0,075) versus the SH

(0,705 ± 0,068) ($p < 0.05$). The total brain p-GSK-3β (Ser-21) levels were significantly increased in the ADZ (0,837 ± 0,084) versus the AD ($p < 0.01$). Although a slight increase was seen in the total brain p-GSK-3β (Ser-21) levels of the SHZ (0,850 ± 0.053) group vs the SH group. This increment did not reach the significance level. No statistically significant difference was observed between the ADZ and SH groups.

# Hippocampus p-GSK-3β (Ser-21) Levels

Mean values of hippocampus p-GSK-3β (Ser-21) levels are given in Fig. 2F. There was a statistically significant difference in hippocampus p-GSK-3β (Ser-21) levels between groups [$F(3,28) = 9.90$, $p < 0.001$]. The hippocampus p-GSK-3β (Ser-21) levels were significantly decreased in the AD (0,467 ± 0,030) versus the SH (0,747 ± 0,068) ($p < 0.001$). The hippocampus p-GSK-3β (Ser-21) levels were significantly increased in the ADZ (0,701 ± 0,023) versus the AD ($p < 0.05$). Although a slight increase was seen in the hippocampus p-GSK-3β (Ser-21) levels of the SHZ (0,805 ± 0.051) group vs the SH group. This increment did not reach the significance level. No statistically significant difference was observed between the ADZ and SH groups.

# Total Brain IDE Levels

Mean values of total brain IDE levels are given in Fig. 3A. There was not a statistically significant difference in total brain IDE levels between groups. Although a slight decrease was seen in the total brain IDE levels of the AD group vs the SH group. This decrement did not reach the significance level. Although a slight increase was seen in the total brain IDE levels of the SHZ group vs the SH group. This increment did not reach the significance level. Although a slight increase was seen in the total brain IDE levels of the ADZ group vs the AD group. This increment did not reach the significance level.

# Hippocampus IDE Levels

Mean values of hippocampus IDE levels are given in Fig. 3B. There was a statistically significant difference in hippocampus IDE levels between groups [$F(3,20) = 47.70$, $p < 0.001$]. The hippocampus IDE levels were significantly decreased in the AD (0,723 ± 0.019) versus the SH (0,890 ± 0,025). The hippocampus IDE levels were significantly increased in the SHZ (1,080 ± 0,031) versus the SH($p < 0.001$ for all comparisons). Although a slight increase was seen in the hippocampus IDE levels of the ADZ group vs the AD group. This increment did not reach the significance level.

# Total Brain NEP Levels

Mean values of total brain NEP levels are given in Fig. 3C. There was a statistically significant difference in total brain NEP levels between groups [$F(3,24) = 12.80$, $p < 0.001$]. The total brain NEP levels were significantly decreased in the AD (0,281 ± 0,033) versus the SH (0,450 ± 0,036) ($p < 0.05$). The total brain NEP levels were significantly increased in the SHZ (0,604 ± 0,048) versus the SH and AD ($p < 0.001$). The total brain NEP levels were significantly increased in the ADZ (0,460 ± 0,024) versus the AD ($p < 0.05$). No statistically significant difference was observed between the ADZ and SH groups.

# Hippocampus NEP Levels

Mean values of hippocampus NEP levels are given in Fig. 3D. There was not a statistically significant difference in hippocampus NEP levels between groups. Although a slight decrease was seen in the hippocampus NEP levels of the AD group vs the SH group. This decrement did not reach the significance level. No statistically significant difference was observed between the SHZ and SH groups. Although a slight increase was seen in the hippocampus NEP levels of the ADZ group vs the AD group. This increment did not reach the significance level.

# Object Recognition Memory Discrimination Index

Object recognition memory discrimination index is given in Fig. 4A. There was a statistically significant difference between groups [$F(3,40) = 70.28$, $p < 0.001$]. The object recognition memory discrimination index was significantly decreased in the AD (8,953 ± 2,625) versus the SH (56,943 ± 3,504). The new object recognition memory discrimination index was significantly increased in the ADZ (75,262 ± 4,032) versus the AD ($p < 0.001$ for all comparisons). Although a slight increase was seen in the new object recognition memory discrimination index of the SHZ group vs the SH group. This increment did not reach the significance level.

# Object Location Memory Discrimination Index

Object location memory discrimination index is given in Fig. 4B. There was a statistically significant difference between groups [$F(3,36) = 47.53$, $p < 0.001$]. The object location memory discrimination index was significantly decreased in the AD (10,343 ± 3,437) versus the SH (49,895 ± 2,633) ($p < 0.001$). The object location memory discrimination index was significantly increased in the ADZ (55,374 ± 4,567) versus the AD ($p < 0.001$). The object location memory discrimination index was significantly increased in the SHZ (72,201 ± 4,253) versus the SH ($p < 0.05$). No statistically significant difference was observed between the ADZ and SHZ groups.

# Spontaneous EEG power spectrum

The only change observed was in delta ($p < 0.001$) and spindle ($p < 0.05$) powers, but not in alpha, or beta powers using the repeated measures of ANOVA for the group and electrode location in spontaneous EEG. In this study, we particularly focused on delta and spindle rhythms because significant changes were observed in these frequency bands between the groups. Representative EEG traces, delta and spindle power spectrums are given in Figs. 5A and B, respectively. We evaluated the difference between the groups as global power values, the means of spectral power at the four recording electrodes, for these frequency bands.

# Spontaneous EEG delta power

In this study, there was not a significant difference between the groups in terms of delta power spectrum. However, rANOVA showed a significant interaction effect for group x location [$F(3,52) = 2.13$, $P < 0.001$], indicating that delta power differed between the groups according to the electrode locations. In the left

temporal region, delta power values in the AH, SHZ and AHZ groups were found to be significantly decreased compared to the SH group ($P < 0.001$).

# Spontaneous EEG spindle power

There was a significant difference between the groups in terms of spindle power spectrum [$F(3,52) = 238.26$, $p < 0.05$]. Spindle power values of the SHZ group were found to be significantly greater than those of the SH, AH and AHZ groups. As a result of the analysis of the spindle power values, it was observed that there was a significant difference between the electrode locations ($p < 0.01$). As a result of the Post Hoc Bonferroni test, spindle power values were found to be significantly increased in the frontal regions compared to the temporal regions. Additionally, rANOVA results for group x location showed a significant interaction effect [$F(3,52) = 3.94$, $P < 0.05$], indicating that spindle power differed between the groups according to the electrode locations. In the Post Hoc Bonferroni test, spindle power values of the SHZ group were found to be significantly higher than those of the SH, AH and AHZ groups in all electrode regions (Fp1, Fp2, T3, T4) ($p < 0.01$). At the same time, spindle power values of the SH and AHZ groups were found to be higher than the AH group only in the left temporal region ($p < 0.05$).

# Correlations between object recognition memory discrimination ındex and left temporal (T3) spindle power spectrum

Significant correlations were found between changes of object recognition memory discrimination index and left temporal (T3) spindle power spectrum (Figs. 5C). There was a positive correlation between object recognition memory discrimination index and left temporal (T3) spindle power spectrum (Pearson $r = 0,448$, $p < 0,001$, $N = 53$).

# Correlations between object location memory discrimination ındex and left temporal (T3) spindle power spectrum

Significant correlations were found between changes of object location memory discrimination index and left temporal (T3) spindle power spectrum (Figs. 5D). There was a positive correlation between object location memory discrimination index and left temporal (T3) spindle power spectrum ($r = 0.433$, $p < 0.01$, $N = 50$).

## Discussion

The pathological changes of AD begin 20 years before the appearance of clinical symptoms [35]. With this respect, investigating the pathological changes seen at the early stage of the disease gains importance. Therefore, we used AβOs to induce the changes similar to the early stage of AD pathology. Weight loss, which is often seen in Alzheimer's patients, may be a signal of the disease even before the onset of dementia symptoms. A study has shown that weight loss is the feature of the early stage of AD

[36]. In line with this, we also found a significant weight loss in AD group rats injected with AβOs compared to the SH group. Thus, together with previous findings, it could be concluded that weight loss is one of the early signs of AD.

It is known that insulin resistance or deficiency can alter Aβ accumulation and tau protein phosphorylation at the early-onset AD [1]. At the same time, it has been shown that the HOMA-IR index of patients with mild cognitive impairment (MCI) was significantly higher than the control group [37]. At the same time, it has been shown that the HOMA-IR index, which is an indicator of peripheral insulin resistance, is significantly higher than the control group, even in patients with MCI [38]. In this context, fasting blood glucose and serum insulin levels, which are common markers of peripheral glucose metabolism, were measured in our study and peripheral insulin resistance was determined by the HOMA-IR index. Our data have shown that Aβ oligomer injection significantly increased fasting blood glucose and serum insulin levels in AD rats compared with the SH rats. At the same time, the HOMA-IR index of the AD group was found to be significantly higher than the SH group. Therefore, our findings suggest that peripheral insulin resistance contributes to the pathogenesis of early AD biomarkers and reveal insights into the pathogenesis of AD. At the same time, it is known that chronic peripheral hyperinsulinemia causes downregulation of insulin receptors in the blood brain barrier and reduces the amount of insulin transported to the brain [39]. In parallel, it has been observed that AD patients who have peripheral hyperinsulinemia have lower brain insulin concentrations [40]. In our study, it was shown that the hippocampal insulin level of the AD group was significantly decreased compared to the SH group. Our findings together with previous observations strongly suggest that chronic hyperinsulinemia in AD may induce a decrement in insulin levels in the brain. Insulin and Aβ are known to be amyloidogenic peptides that share a common sequence recognition motif. At the same time, AβOs can bind to insulin receptors and inhibit the phosphorylation of the receptor [13]. In our study, it was planned to examine the effect of AβOs on the insulin signaling pathway in the rat model created by injection of AβOs.

A previous report showed that IRS-1 Ser 612 phosphorylation is decreased along with the reduction in total IRS-1 levels in the early phase of AD disease. Also, it has been shown that IRS-1 Ser612 phosphorylation gradually increases with the progression of the disease. So, it was concluded that this decrease in IRS-1 Ser612 phosphorylation is a defense mechanism that ensures the continuation of the insulin signaling pathway in the early phase of the disease [41]. In our study, we found that total brain IRS-1 Ser612 phosphorylation was significantly decreased in the AD group compared to the SH group. In addition, hippocampus IRS-1 Ser612 phosphorylation was slightly decreased in the AD group, although it did not reach the significance level. Our findings, together with the finding mentioned above, suggest that decrement of brain p-IRS1 Ser612 level occurs at the early stage of AD progression. Therefore, we can conclude that there is an impairment of brain IRS-1 activation at the onset of AD disease.

When IRS-1 complex is activated in the insulin signaling pathway, it activates the PI3K→PKB/Akt pathway which phosphorylates the Ser9/21 region of GSK3β and suppresses the GSK-3β activity [42]. It was shown that insulin resistance or deficiency can change Aβ and tau phosphorylation, thereby, contributing to the onset of AD by overactivity of GSK-3β [43, 44]. We found a marked decrement in p-

GSK-3β Ser21 phosphorylation which was accompanied by the reduction of IRS-1 phosphorylation in the hippocampus and total brain. GSK-3β regulates the binding of tau protein to microtubules [45]. Especially increased tau toxicity associated with Aβ depends on phosphorylation of tau at Ser262/356 sides that decreases the binding of tau protein to microtubules [46]. Consistent with this, we found a significant increase in the p-Tau Ser356 level in the hippocampus of the AD group versus the SH group. In addition, we observed an increament trend in the p-Tau Ser356 level in the total brain in the AD group versus the SH group, but this increase did not reach the level of significance.

In the central nervous system, insulin signaling is required for the expression of genes that modulate memory [41]. Hence, the observed change in the insulin signaling pathway very likely alters the cognitive functions in the current study. We used object recognition and object location memory tests, which are widely used tests to assess memory deficits. Object location memory requires the hippocampus to encode, consolidate, and recall information [47, 48]. According to a recent study, AβOs injections resulted in significant impairment of the object location memory index. In this study, AβOs impair performance in hippocampal-dependent associative learning tasks [49]. Also, AβOs injection resulted in significant impairment of the spatial memory index score for the object location memory test [50]. Consistent with these studies, we found a significant decrease in the object location memory discrimination index in the AD group versus the SH group. Several different brain regions are critical for the new object recognition memory, including the insular cortex [51, 52], the perirhinal cortex [53, 54, 52], and the ventromedial prefrontal cortex [55]. According to a previous study, the object recognition memory discrimination index significantly decreased in the Aβ oligomer-treated mice [50]. In parallel, we found a significant decrease in the new object recognition memory discrimination index in the AD group versus the SH group. Collectively these findings suggest that altered insulin signaling pathway mediated AβOs induced memory dysfunctions during the onset of AD, and ultimately contributor to AD pathology.

Regulation of proteases that degrade Aβ may represent an important therapeutic approach. The two main peptidases that mainly regulate Aβ metabolism in the brain are the enzymes NEP and IDE [56]. It is well known that IDE [57, 58] and NEP [59] levels decrease with aging and at the early stage of AD. In the current study, we found a significant reduction in hippocampus IDE levels in the AD group versus the SH group and a tendency for a reduction in the total brain region, although it was not significant. In addition, we found a significant reduction in total brain NEP levels in the AD group versus the SH group and a tendency for a reduction in the hippocampus, although it was not significant.

It is well known that $Zn^{+2}$ deficiency commonly takes place in AD pathology [24, 25]. Earlier studies indicate that, Cyclo-Z which CHP and $Zn^{+2}$ combination increase absorption of $Zn^{+2}$ [28] and improve weight control [30]. Therefore, firstly, we aimed to investigate how Cyclo-Z affects weight control. We found a significant increase in weight in the ADZ group versus the AD group. Moreover, Cyclo-Z administration decreases fasting blood glucose [60–62], and enhances insulin sensitivity and glucose tolerance [62–64]. We found a significant reduction in fasting blood glucose levels in the ADZ group versus the AD group. In addition, although not significant, we found a tendency for a reduction in the HOMA-IR index and serum insulin levels in the ADZ group versus the AD group. When the hippocampus

insulin levels were examined, no significant difference was found in the ADZ group. Therefore, in our study, Cyclo-Z was found to have a possible positive effect on weight loss, peripheral insulin resistance and brain insulin levels in the ADZ rats. However, we found a tendency for a reduction in the weight in the SHZ group versus the SH group. This reduction can be explained by $Zn^{+2}$ toxicity. An overdose of $Zn^{+2}$ has been shown to have a toxic potential in humans in a previous study [65]. At the same time, fasting blood glucose levels, serum insulin levels and HOMA-IR index also increased and hippocampal insulin levels decreased in the SHZ group versus SH group. These results strongly demonstrate that $Zn^{+2}$ toxicity not only has a side effect on weight control but also leads to peripheral insulin resistance and a decrease in brain insulin levels.

The effect of Cyclo-Z on the brain insulin signaling pathway was also investigated in our study. Ser phosphorylation of IRS-1 might negatively or positively regulate insulin signaling, depending on the sites where it occurs. If insulin phosphorylates IRS-1 on Ser residues, insulin signaling is desensitized and adversely affected. However, the insulin signaling pathway is positively regulated if PKB/Akt phosphorylates IRS-1 over Ser residues. IRS-1 proteins have four Ser residues that act as PKB/Akt phosphorylation sites, and Ser612 is one of them. When insulin signaling is activated for a long time, it overexpresses PKB/Akt and phosphorylates IRS-1 from these Ser sites. Increased IRS-1 Ser612 phosphorylation protects IRS-1 from the rapid action of tyrosine phosphatases and keeps it in its phosphorylated active form [66]. In line, we found a significant increase in hippocampal and brain p-IRS-1 Ser612 levels in the ADZ group compared to the AD group. Therefore, we concluded that p-IRS-1 Ser612 phosphorylation was increased in ADZ group animals due to long-term activation of insulin signaling. Similar results were found in the p-IRS-1 Ser612 level of the SHZ group, which was seen to have improved insulin signal due to Cyclo-Z treatment. We found a significant decrease in the hippocampal p-IRS-1 Ser612 level in the SHZ group versus the SH group. There was also a trend towards an increase in the total brain p-IRS-1 Ser612 level, although this was not significant. The downstream target, p-GSK-3β Ser21, was also examined to reveal the changes in the insulin signaling pathway. We found a significant increase in the hippocampal and total brain p-GSK-3β Ser21 levels in the ADZ group versus the AD group. In addition, we found a significant decrease in hippocampal p-GSK-3β Ser-21 levels in the SHZ group compared to the SH group. In addition, although total brain p-GSK-3β Ser-21 phosphorylation was decreased in the SHZ group compared to the SH group, it did not reach a significant level. It is well known from previous studies that $Zn^{+2}$ has insulin-like effects and facilitates insulin signaling [22]. These effects are largely dependent on the activation of PKB/Akt signaling [67]. Therefore, we suggest that Cyclo-Z showed a facilitatory effect on the brain insulin pathway in SHZ and ADZ groups.

The effects of Cyclo-Z treatment on AβO and tau protein phosphorylation were also investigated. We found a significant decrease in AβO levels in the ADZ group versus the AD group in both regions. Whereas, we found that there was a significant increase in p-Tau Ser356 levels in both regions of ADZ group rats compared to the AD group. We presume that other possible mechanisms which contribute to the AD pathophysiology may play a role in the increased p-Tau Ser356 levels. GSK-3β and protein phosphatase 2A (PP2A) are important enzymes that control tau hyperphosphorylation. The relationship

between these two enzymes and their effect on tau hyperphosphorylation is not yet fully understood. In a study, it was found that GSK-3β and PP2A regulate each other and regulate tau phosphorylation directly and indirectly through modulation of each other [42]. Inactivation of GSK-3β resulting from PI3K-AKT activation has been shown to lead to PP2A demethylation and inactivation, resulting in tau hyperphosphorylation. Based on these results, we suggest that targeting GSK-3β could lead to an increment of tau phosphorylation in Ser262/356, which is one of the PP2A sensitive regions. In line, it has been suggested that the Ser262/356 region required for tau pathology is specific for PP2A and that PP2A should be addressed as the therapeutic target for tau pathology [42]. So, while Cyclo-Z treatment decreased the GSK-3β activity in the AHZ group, it could not reduce the p-Tau Ser356 levels in the current study.

Although the Cyclo-Z agent was found to decrease the AβOs level in the ADZ group, it was shown that the AβOs level of the SHZ group were significantly increased in all regions compared to the SH group. When Cyclo-Z agent administered to healthy rats, it had a negative effect on AβOs level. It is known that aggregation of Aβ peptides can be rapidly induced in the presence of $Zn^{+2}$ ions under physiological conditions in vitro. It has abeen shown that $Zn^{+2}$ ions coexist with Aβ deposits. Although the $Zn^{+2}$ concentration required for fibrillation is controversial, it certainly has an important role in Aβ aggregation [26]. So, it is rational that Cyclo-Z treatment in healthy rats increases AβOs level, as high $Zn^{+2}$ ion concentrations are also known to induce Aβ aggregation and tau protein modification [68]. Although not significant, Cyclo-Z agent tended to increase the p-Tau Ser356 levels of the SHZ group compared to the SH group. Therefore, we suggest that excessive $Zn^{+2}$ supplementation may cause AD-like toxicities.

Additionally, we used memory tests to examine the effect of Cyclo-Z treatment on cognitive functions. We found a significant increase in discriminative index of object recognition test in the ADZ group versus the AD group. At the same time, we found a tendency for an increment in the SHZ group versus the SH group but did not reach the significance level. Likewise, we found a significant increment in the discriminative index of object location test in the ADZ group versus the AD group. Discriminative index of object location test showed a similar increment in the SHZ group versus the SH group.

It is a known fact that IDE and NEP enzymes, which are known to degrade Aβ [69], require $Zn^{+2}$ for both gene expression and activity [26]. Thus, $Zn^{+2}$ supplementation can induce the synthesis of these Aβ-clearing enzymes [23]. At the same time, it has been suggested in previous studies that Cyclo-Z is the only agent that can increase intracellular IDE [62, 63]. Therefore, in our study, the effect of Cyclo-Z on IDE and NEP enzymes was also investigated. Our data have shown that Cyclo-Z treatment significantly increased hippocampal and total brain IDE and NEP levels in the ADZ group versus the AD group. Also, we found a significant increase in hippocampal and total brain IDE and NEP levels in the SHZ group versus the SH group. Our findings together with previous observations strongly suggest that Cyclo-Z has a positive effect on Aβ degradation by increasing the amount of IDE and NEP enzymes.

Accumulating evidence indicates that AβOs exposure induces changes in presynaptic and postsynaptic synapses. AβOs are likely to induce changes in neural network dynamics. For this reason, in our study, we

investigated the effects of AβOs on neural network dynamics under ketamine anesthesia using the EEG technique. It is well known that spontaneous EEG under ketamine anesthesia mimics sleeping EEG patterns [70], and AD pathophysiology markedly disrupted sleeping physiology [71]. Moreover, it was evidenced that Alzheimer's patients showed reduced spindle density and spindle activity [72]. An early study also indicated that AD pathology diminished cortical spindle power in APP/PS1 Tg mice [73]. Consistent with aforementioned studies, we found that the left temporal region (T3) spindle power was significantly reduced in the AD group compared to the SH group. Hence, we can conclude that the diminished spindle power spectrum in the left temporal region reveals insights into the pathogenesis of AD. In addition, we found a significant increase in temporal spindle spectral power values in the ADZ group versus the SH group. At the same time, the spindle power values of the SHZ group were significantly higher than SH, AD and ADZ in all electrode regions. Although AβO and tau pathology was observed in the SHZ group, Cyclo-Z treatment increased spindle power values in all electrode areas. In line with this, adequate $Zn^{+2}$ concentration is known to improve sleep quality [74]. A previous study has also shown that increased spindle power contributes to sleep quality with significant effects on memory consolidation [71]. Consistent with this, we found a positive correlation between left temporal (T3) spindle power and new object discrimination index (Pearson r = 0,448, $p < 0.001$, N = 53), and location discrimination index (Pearson r = 0,433, $p < 0.01$, N = 50). From this point of view, it could be concluded that Cyclo-Z might increase spindle formation left temporal region and memory consolidation. It has been noted that slow brain waves are impaired in the presence of AβOs before the deposition of Aβ plaques [75]. Additionally, it was shown that reduced delta power has a relation with increased tau deposits [76]. In the left temporal region, delta power values in the SHZ, AD and ADZ groups were found to be significantly decreased compared to the SH group. The decrease of delta power in the SHZ group might be associated with the AβOs toxicity and tau pathology depending on $Zn^{+2}$ toxicity. In addition, although sleep delta spectral power was increased in the ADZ group versus the AD group, it did not reach the significance level.

# Conclusions

In conclusion, our results are consistent with previous findings that weight loss, peripheral hyperinsulinemia, and peripheral insulin resistance may play a central role in the early stage of AD. In addition, it can be concluded that peripheral hyperinsulinemia seen in the early phase of AD may decrease the hippocampal insulin level. Furthermore, decreament of brain insulin levels may also cause dysregulation of brain insulin pathway. These changes have also been shown to reduce the levels of IDE and NEP that exacerbate AβOs toxicity and may play a role in increased p-Tau Ser356. Furthermore, AβOs impair memory functions and network dynamics by altering the brain's insulin signal pathway in the early stage of AD, and ultimately contributor to AD pathology. The Cyclo-Z treatment was found to have a positive effect on weight loss, peripheral insulin resistance, and brain insulin level. Cyclo-Z treatment to AD rats increased the levels of amyloid-degrading enzymes and reduced AβOs accumulation. At the same time, the Cyclo-Z agent applied to ADZ rats could not prevent the increase of p-Tau Ser 356 level. However, it was observed that the Cyclo-Z agent applied to healthy animals had a negative effect due to

$Zn^{+2}$ toxicity. Cyclo-Z treatment in healthy animals increased the level of amyloid-degrading enzymes but resulted in the accumulation of AβOs. It was thought that this increase observed in AβOs accumulation may be caused by $Zn^{+2}$ toxicity. At the same time, it was found that the p-Tau Ser356 level was similarly increased due to the toxicity. Cyclo-Z treatment was found to have positive effects on new object recognition and location memory functions in healthy and AD group rats. Besides, Cyclo-Z treatment was found to have a significant positive effect on spindle power and slightly increased the delta power in the left temporal region. In sum, agents that improve insulin delivery, such as Cyclo-Z, may be an important therapeutic approach to prevent various pathological processes in the early stage of AD.

# Declarations


### Acknowledgements

Not applicable

### Funding

This study was supported by a grant from Akdeniz University Research Foundation, Turkey (Grant No: TDK-2018-3272).


### Competing Interests

The authors declare that they have no competing interests.

### Author Contributions

ADA, DK and HE generated the rat models, recording and analyses of EEG, and were involved in the study design. ADA and OE analyzed the western blot datas. All the authors previously mentioned, as well as ND and PY, were involved in data interpretation, critically reviewed and provided their fnal approval to the manuscript, and agree to be accountable for the work.

### Data Availability

All data is real and guarantees the validity of experimental results.

### Ethics Approval

Ethical approval for this work was obtained from Akdeniz University Local Committee on Animal Research Ethics (ethics approval date and number: 26.01.2018/2018.01.014-17).

### Consent to Participate

Not applicable.

### Consent to Publish

Not appicable.

### Conflict of İnterest

The authors report no conflicts of interest in this work.

# References


1. Song MK, Bischoff DS, Song AM, Uyemura K, Yamaguchi DT (2017) Metabolic relationship between diabetes and Alzheimer's Disease affected by Cyclo(His-Pro) plus zinc treatment. BBA Clin 7:41-54. doi:10.1016/j.bbacli.2016.09.003
2. Lambert MP, Barlow AK, Chromy BA, Edwards C, Freed R, Liosatos M, Morgan TE, Rozovsky I, Trommer B, Viola KL, Wals P, Zhang C, Finch CE, Krafft GA, Klein WL (1998) Diffusible, nonfibrillar ligands derived from Abeta1-42 are potent central nervous system neurotoxins. Proc Natl Acad Sci U S A 95 (11):6448-6453
3. Walsh DM, Klyubin I, Fadeeva JV, Cullen WK, Anwyl R, Wolfe MS, Rowan MJ, Selkoe DJ (2002) Naturally secreted oligomers of amyloid beta protein potently inhibit hippocampal long-term potentiation in vivo. Nature 416 (6880):535-539. doi:10.1038/416535a 416535a [pii]
4. Shankar GM, Li S, Mehta TH, Garcia-Munoz A, Shepardson NE, Smith I, Brett FM, Farrell MA, Rowan MJ, Lemere CA, Regan CM, Walsh DM, Sabatini BL, Selkoe DJ (2008) Amyloid-beta protein dimers isolated directly from Alzheimer's brains impair synaptic plasticity and memory. Nat Med 14 (8):837-842. doi:nm1782 [pii]10.1038/nm1782
5. Lesne S, Koh MT, Kotilinek L, Kayed R, Glabe CG, Yang A, Gallagher M, Ashe KH (2006) A specific amyloid-beta protein assembly in the brain impairs memory. Nature 440 (7082):352-357. doi:nature04533 [pii]10.1038/nature04533
6. Miyauchi T, Hagimoto H, Ishii M, Endo S, Tanaka K, Kajiwara S, Endo K, Kajiwara A, Kosaka K (1994) Quantitative EEG in patients with presenile and senile dementia of the Alzheimer type. Acta Neurol Scand 89 (1):56-64
7. Brunovsky M, Matousek M, Edman A, Cervena K, Krajca V (2003) Objective assessment of the degree of dementia by means of EEG. Neuropsychobiology 48 (1):19-26. doi:10.1159/000071824
8. de la Monte SM, Wands JR (2005) Review of insulin and insulin-like growth factor expression, signaling, and malfunction in the central nervous system: relevance to Alzheimer's disease. J Alzheimers Dis 7 (1):45-61. doi:10.3233/jad-2005-7106
9. Schuh AF, Rieder CM, Rizzi L, Chaves M, Roriz-Cruz M (2011) Mechanisms of brain aging regulation by insulin: implications for neurodegeneration in late-onset Alzheimer's disease. ISRN Neurol 2011:306905. doi:10.5402/2011/306905
10. Haass C, Selkoe DJ (2007) Soluble protein oligomers in neurodegeneration: lessons from the Alzheimer's amyloid beta-peptide. Nat Rev Mol Cell Biol 8 (2):101-112. doi:10.1038/nrm2101

11. Ferreira ST, Vieira MN, De Felice FG (2007) Soluble protein oligomers as emerging toxins in Alzheimer's and other amyloid diseases. IUBMB Life 59 (4-5):332-345. doi:10.1080/15216540701283882
12. Ferreira ST, Klein WL (2011) The Abeta oligomer hypothesis for synapse failure and memory loss in Alzheimer's disease. Neurobiol Learn Mem 96 (4):529-543. doi:10.1016/j.nlm.2011.08.003
13. Xie L, Helmerhorst E, Taddei K, Plewright B, Van Bronswijk W, Martins R (2002) Alzheimer's beta-amyloid peptides compete for insulin binding to the insulin receptor. J Neurosci 22 (10):RC221. doi:20026383
14. Zhao WQ, De Felice FG, Fernandez S, Chen H, Lambert MP, Quon MJ, Krafft GA, Klein WL (2008) Amyloid beta oligomers induce impairment of neuronal insulin receptors. FASEB J 22 (1):246-260. doi:10.1096/fj.06-7703com
15. De Felice FG, Vieira MN, Bomfim TR, Decker H, Velasco PT, Lambert MP, Viola KL, Zhao WQ, Ferreira ST, Klein WL (2009) Protection of synapses against Alzheimer's-linked toxins: insulin signaling prevents the pathogenic binding of Abeta oligomers. Proc Natl Acad Sci U S A 106 (6):1971-1976. doi:10.1073/pnas.0809158106
16. Lane RF, Shineman DW, Steele JW, Lee LB, Fillit HM (2012) Beyond amyloid: the future of therapeutics for Alzheimer's disease. Adv Pharmacol 64:213-271. doi:10.1016/B978-0-12-394816-8.00007-6
17. Lacor PN, Buniel MC, Furlow PW, Clemente AS, Velasco PT, Wood M, Viola KL, Klein WL (2007) Abeta oligomer-induced aberrations in synapse composition, shape, and density provide a molecular basis for loss of connectivity in Alzheimer's disease. J Neurosci 27 (4):796-807. doi:10.1523/JNEUROSCI.3501-06.2007
18. Escribano L, Simon AM, Gimeno E, Cuadrado-Tejedor M, Lopez de Maturana R, Garcia-Osta A, Ricobaraza A, Perez-Mediavilla A, Del Rio J, Frechilla D (2010) Rosiglitazone rescues memory impairment in Alzheimer's transgenic mice: mechanisms involving a reduced amyloid and tau pathology. Neuropsychopharmacology 35 (7):1593-1604. doi:10.1038/npp.2010.32
19. Jha NK, Jha SK, Kumar D, Kejriwal N, Sharma R, Ambasta RK, Kumar P (2015) Impact of Insulin Degrading Enzyme and Neprilysin in Alzheimer's Disease Biology: Characterization of Putative Cognates for Therapeutic Applications. J Alzheimers Dis 48 (4):891-917. doi:10.3233/JAD-150379
20. Pivovarova O, Hohn A, Grune T, Pfeiffer AF, Rudovich N (2016) Insulin-degrading enzyme: new therapeutic target for diabetes and Alzheimer's disease? Ann Med 48 (8):614-624. doi:10.1080/07853890.2016.1197416
21. Morales-Corraliza J, Wong H, Mazzella MJ, Che S, Lee SH, Petkova E, Wagner JD, Hemby SE, Ginsberg SD, Mathews PM (2016) Brain-Wide Insulin Resistance, Tau Phosphorylation Changes, and Hippocampal Neprilysin and Amyloid-beta Alterations in a Monkey Model of Type 1 Diabetes. J Neurosci 36 (15):4248-4258. doi:10.1523/JNEUROSCI.4640-14.2016
22. Miao X, Sun W, Fu Y, Miao L, Cai L (2013) Zinc homeostasis in the metabolic syndrome and diabetes. Front Med 7 (1):31-52. doi:10.1007/s11684-013-0251-9

23. Lifshitz V, Benromano T, Weiss R, Blanga-Kanfi S, Frenkel D (2013) Insulin-degrading enzyme deficiency accelerates cerebrovascular amyloidosis in an animal model. Brain Behav Immun 30:143-149. doi:10.1016/j.bbi.2012.12.003
24. Roberts RO, Knopman DS, Geda YE, Cha RH, Pankratz VS, Baertlein L, Boeve BF, Tangalos EG, Ivnik RJ, Mielke MM, Petersen RC (2014) Association of diabetes with amnestic and nonamnestic mild cognitive impairment. Alzheimers Dement 10 (1):18-26. doi:10.1016/j.jalz.2013.01.001
25. Afkarian M, Zelnick LR, Hall YN, Heagerty PJ, Tuttle K, Weiss NS, de Boer IH (2016) Clinical Manifestations of Kidney Disease Among US Adults With Diabetes, 1988-2014. JAMA 316 (6):602-610. doi:10.1001/jama.2016.10924
26. Watt NT, Whitehouse IJ, Hooper NM (2010) The role of zinc in Alzheimer's disease. Int J Alzheimers Dis 2011:971021. doi:10.4061/2011/971021
27. Borza DB, Morgan WT (1998) Histidine-proline-rich glycoprotein as a plasma pH sensor. Modulation of its interaction with glycosaminoglycans by ph and metals. J Biol Chem 273 (10):5493-5499. doi:10.1074/jbc.273.10.5493
28. Rosenthal MJ, Hwang IK, Song MK (2001) Effects of arachidonic acid and cyclo (his-pro) on zinc transport across small intestine and muscle tissues. Life Sci 70 (3):337-348. doi:10.1016/s0024-3205(01)01395-9
29. Maher PA, Schubert DR (2009) Metabolic links between diabetes and Alzheimer's disease. Expert Rev Neurother 9 (5):617-630. doi:10.1586/ern.09.18
30. Song MK, Rosenthal MJ, Song AM, Uyemura K, Yang H, Ament ME, Yamaguchi DT, Cornford EM (2009) Body weight reduction in rats by oral treatment with zinc plus cyclo-(His-Pro). Br J Pharmacol 158 (2):442-450. doi:10.1111/j.1476-5381.2009.00201.x
31. Wang X, Hu X, Yang Y, Takata T, Sakurai T (2015) Systemic pyruvate administration markedly reduces neuronal death and cognitive impairment in a rat model of Alzheimer's disease. Exp Neurol 271:145-154. doi:10.1016/j.expneurol.2015.06.008
32. Li Y, Duffy KB, Ottinger MA, Ray B, Bailey JA, Holloway HW, Tweedie D, Perry T, Mattson MP, Kapogiannis D, Sambamurti K, Lahiri DK, Greig NH (2010) GLP-1 receptor stimulation reduces amyloid-beta peptide accumulation and cytotoxicity in cellular and animal models of Alzheimer's disease. J Alzheimers Dis 19 (4):1205-1219. doi:10.3233/JAD-2010-1314
33. Gong L, Li SL, Li H, Zhang L (2011) Ginsenoside Rg1 protects primary cultured rat hippocampal neurons from cell apoptosis induced by beta-amyloid protein. Pharm Biol 49 (5):501-507. doi:10.3109/13880209.2010.521514
34. Roozendaal B, Hernandez A, Cabrera SM, Hagewoud R, Malvaez M, Stefanko DP, Haettig J, Wood MA (2010) Membrane-associated glucocorticoid activity is necessary for modulation of long-term memory via chromatin modification. J Neurosci 30 (14):5037-5046. doi:10.1523/JNEUROSCI.5717-09.2010
35. Kshirsagar V, Thingore C, Juvekar A (2021) Insulin resistance: a connecting link between Alzheimer's disease and metabolic disorder. Metab Brain Dis 36 (1):67-83. doi:10.1007/s11011-020-00622-2

36. James D, Kang S, Park S (2014) Injection of beta-amyloid into the hippocampus induces metabolic disturbances and involuntary weight loss which may be early indicators of Alzheimer's disease. Aging Clin Exp Res 26 (1):93-98. doi:10.1007/s40520-013-0181-z
37. Craft S, Newcomer J, Kanne S, Dagogo-Jack S, Cryer P, Sheline Y, Luby J, Dagogo-Jack A, Alderson A (1996) Memory improvement following induced hyperinsulinemia in Alzheimer's disease. Neurobiol Aging 17 (1):123-130. doi:10.1016/0197-4580(95)02002-0
38. Zhao H, Wu C, Zhang X, Wang L, Sun J, Zhuge F (2019) Insulin Resistance Is a Risk Factor for Mild Cognitive Impairment in Elderly Adults with T2DM. Open Life Sci 14:255-261. doi:10.1515/biol-2019-0029
39. Sano H, Eguez L, Teruel MN, Fukuda M, Chuang TD, Chavez JA, Lienhard GE, McGraw TE (2007) Rab10, a target of the AS160 Rab GAP, is required for insulin-stimulated translocation of GLUT4 to the adipocyte plasma membrane. Cell Metab 5 (4):293-303. doi:10.1016/j.cmet.2007.03.001
40. Rui L (2014) Energy metabolism in the liver. Compr Physiol 4 (1):177-197. doi:10.1002/cphy.c130024
41. Velazquez R, Tran A, Ishimwe E, Denner L, Dave N, Oddo S, Dineley KT (2017) Central insulin dysregulation and energy dyshomeostasis in two mouse models of Alzheimer's disease. Neurobiol Aging 58:1-13. doi:10.1016/j.neurobiolaging.2017.06.003
42. Wang Y, Yang R, Gu J, Yin X, Jin N, Xie S, Wang Y, Chang H, Qian W, Shi J, Iqbal K, Gong CX, Cheng C, Liu F (2015) Cross talk between PI3K-AKT-GSK-3beta and PP2A pathways determines tau hyperphosphorylation. Neurobiol Aging 36 (1):188-200. doi:10.1016/j.neurobiolaging.2014.07.035
43. Lauretti E, Dincer O, Pratico D (2020) Glycogen synthase kinase-3 signaling in Alzheimer's disease. Biochim Biophys Acta Mol Cell Res 1867 (5):118664. doi:10.1016/j.bbamcr.2020.118664
44. Li X, Song D, Leng SX (2015) Link between type 2 diabetes and Alzheimer's disease: from epidemiology to mechanism and treatment. Clin Interv Aging 10:549-560. doi:10.2147/CIA.S74042
45. Ahmad W (2013) Overlapped metabolic and therapeutic links between Alzheimer and diabetes. Mol Neurobiol 47 (1):399-424. doi:10.1007/s12035-012-8352-z
46. Ando K, Maruko-Otake A, Ohtake Y, Hayashishita M, Sekiya M, Iijima KM (2016) Stabilization of Microtubule-Unbound Tau via Tau Phosphorylation at Ser262/356 by Par-1/MARK Contributes to Augmentation of AD-Related Phosphorylation and Abeta42-Induced Tau Toxicity. PLoS Genet 12 (3):e1005917. doi:10.1371/journal.pgen.1005917
47. Mumby DG, Gaskin S, Glenn MJ, Schramek TE, Lehmann H (2002) Hippocampal damage and exploratory preferences in rats: memory for objects, places, and contexts. Learn Mem 9 (2):49-57. doi:10.1101/lm.41302
48. Haettig J, Stefanko DP, Multani ML, Figueroa DX, McQuown SC, Wood MA (2011) HDAC inhibition modulates hippocampus-dependent long-term memory for object location in a CBP-dependent manner. Learn Mem 18 (2):71-79. doi:10.1101/lm.1986911
49. Rozema NB, Procissi D, Bertolino N, Viola KL, Nandwana V, Abdul N, Pribus S, Dravid V, Klein WL, Disterhoft JF, Weiss C (2020) Abeta oligomer induced cognitive impairment and evaluation of ACU193-MNS-based MRI in rabbit. Alzheimers Dement (N Y) 6 (1):e12087. doi:10.1002/trc2.12087

50. Kim DH, Choi SM, Jho J, Park MS, Kang J, Park SJ, Ryu JH, Jo J, Kim HH, Kim BC (2016) Infliximab ameliorates AD-associated object recognition memory impairment. Behav Brain Res 311:384-391. doi:10.1016/j.bbr.2016.06.001
51. Bermudez-Rattoni F, Okuda S, Roozendaal B, McGaugh JL (2005) Insular cortex is involved in consolidation of object recognition memory. Learn Mem 12 (5):447-449. doi:10.1101/lm.97605
52. Balderas I, Rodriguez-Ortiz CJ, Salgado-Tonda P, Chavez-Hurtado J, McGaugh JL, Bermudez-Rattoni F (2008) The consolidation of object and context recognition memory involve different regions of the temporal lobe. Learn Mem 15 (9):618-624. doi:10.1101/lm.1028008
53. Winters BD, Forwood SE, Cowell RA, Saksida LM, Bussey TJ (2004) Double dissociation between the effects of peri-postrhinal cortex and hippocampal lesions on tests of object recognition and spatial memory: heterogeneity of function within the temporal lobe. J Neurosci 24 (26):5901-5908. doi:10.1523/JNEUROSCI.1346-04.2004
54. Winters BD, Bussey TJ (2005) Transient inactivation of perirhinal cortex disrupts encoding, retrieval, and consolidation of object recognition memory. J Neurosci 25 (1):52-61. doi:10.1523/JNEUROSCI.3827-04.2005
55. Akirav I, Maroun M (2006) Ventromedial prefrontal cortex is obligatory for consolidation and reconsolidation of object recognition memory. Cereb Cortex 16 (12):1759-1765. doi:10.1093/cercor/bhj114
56. Yamamoto N, Ishikuro R, Tanida M, Suzuki K, Ikeda-Matsuo Y, Sobue K (2018) Insulin-signaling Pathway Regulates the Degradation of Amyloid beta-protein via Astrocytes. Neuroscience 385:227-236. doi:10.1016/j.neuroscience.2018.06.018
57. Zhao Z, Xiang Z, Haroutunian V, Buxbaum JD, Stetka B, Pasinetti GM (2007) Insulin degrading enzyme activity selectively decreases in the hippocampal formation of cases at high risk to develop Alzheimer's disease. Neurobiol Aging 28 (6):824-830. doi:10.1016/j.neurobiolaging.2006.05.001
58. Stargardt A, Gillis J, Kamphuis W, Wiemhoefer A, Kooijman L, Raspe M, Benckhuijsen W, Drijfhout JW, Hol EM, Reits E (2013) Reduced amyloid-beta degradation in early Alzheimer's disease but not in the APPswePS1dE9 and 3xTg-AD mouse models. Aging Cell 12 (3):499-507. doi:10.1111/acel.12074
59. Sikanyika NL, Parkington HC, Smith AI, Kuruppu S (2019) Powering Amyloid Beta Degrading Enzymes: A Possible Therapy for Alzheimer's Disease. Neurochem Res 44 (6):1289-1296. doi:10.1007/s11064-019-02756-x
60. Song MK, Rosenthal MJ, Naliboff BD, Phanumas L, Kang KW (1998) Effects of bovine prostate powder on zinc, glucose, and insulin metabolism in old patients with non-insulin-dependent diabetes mellitus. Metabolism 47 (1):39-43. doi:10.1016/s0026-0495(98)90190-1
61. Song MK, Rosenthal MJ, Hong S, Harris DM, Hwang I, Yip I, Golub MS, Ament ME, Go VL (2001) Synergistic antidiabetic activities of zinc, cyclo (his-pro), and arachidonic acid. Metabolism 50 (1):53-59. doi:10.1053/meta.2001.19427
62. Hwang IK, Go VL, Harris DM, Yip I, Kang KW, Song MK (2003) Effects of cyclo (his-pro) plus zinc on glucose metabolism in genetically diabetic obese mice. Diabetes Obes Metab 5 (5):317-324.

doi:10.1046/j.1463-1326.2003.00281.x

63. Song MK, Hwang IK, Rosenthal MJ, Harris DM, Yamaguchi DT, Yip I, Go VL (2003) Anti-hyperglycemic activity of zinc plus cyclo (his-pro) in genetically diabetic Goto-Kakizaki and aged rats. Exp Biol Med (Maywood) 228 (11):1338-1345. doi:10.1177/153537020322801112
64. Song MK, Rosenthal MJ, Song AM, Yang H, Ao Y, Yamaguchi DT (2005) Raw vegetable food containing high cyclo (his-pro) improved insulin sensitivity and body weight control. Metabolism 54 (11):1480-1489. doi:10.1016/j.metabol.2005.05.014
65. Yeh YH, Lee YT, Hsieh YL, Hwang DF (2011) Dietary taurine reduces zinc-induced toxicity in male Wistar rats. J Food Sci 76 (4):T90-98. doi:10.1111/j.1750-3841.2011.02110.x
66. Paz K, Liu YF, Shorer H, Hemi R, LeRoith D, Quan M, Kanety H, Seger R, Zick Y (1999) Phosphorylation of insulin receptor substrate-1 (IRS-1) by protein kinase B positively regulates IRS-1 function. J Biol Chem 274 (40):28816-28822. doi:10.1074/jbc.274.40.28816
67. Sun W, Yang J, Wang W, Hou J, Cheng Y, Fu Y, Xu Z, Cai L (2018) The beneficial effects of Zn on Akt-mediated insulin and cell survival signaling pathways in diabetes. J Trace Elem Med Biol 46:117-127. doi:10.1016/j.jtemb.2017.12.005
68. Kabir MT, Uddin MS, Zaman S, Begum Y, Ashraf GM, Bin-Jumah MN, Bungau SG, Mousa SA, Abdel-Daim MM (2021) Molecular Mechanisms of Metal Toxicity in the Pathogenesis of Alzheimer's Disease. Mol Neurobiol 58 (1):1-20. doi:10.1007/s12035-020-02096-w
69. Shirotani K, Tsubuki S, Iwata N, Takaki Y, Harigaya W, Maruyama K, Kiryu-Seo S, Kiyama H, Iwata H, Tomita T, Iwatsubo T, Saido TC (2001) Neprilysin degrades both amyloid beta peptides 1-40 and 1-42 most rapidly and efficiently among thiorphan- and phosphoramidon-sensitive endopeptidases. J Biol Chem 276 (24):21895-21901. doi:10.1074/jbc.M008511200
70. Lazarewicz MT, Ehrlichman RS, Maxwell CR, Gandal MJ, Finkel LH, Siegel SJ (2010) Ketamine modulates theta and gamma oscillations. J Cogn Neurosci 22 (7):1452-1464. doi:10.1162/jocn.2009.21305
71. Ladenbauer J, Ladenbauer J, Kulzow N, de Boor R, Avramova E, Grittner U, Floel A (2017) Promoting Sleep Oscillations and Their Functional Coupling by Transcranial Stimulation Enhances Memory Consolidation in Mild Cognitive Impairment. J Neurosci 37 (30):7111-7124. doi:10.1523/JNEUROSCI.0260-17.2017
72. Mander BA (2020) Local Sleep and Alzheimer's Disease Pathophysiology. Front Neurosci 14:525970. doi:10.3389/fnins.2020.525970
73. Zhurakovskaya E, Ishchenko I, Gureviciene I, Aliev R, Grohn O, Tanila H (2019) Impaired hippocampal-cortical coupling but preserved local synchrony during sleep in APP/PS1 mice modeling Alzheimer's disease. Sci Rep 9 (1):5380. doi:10.1038/s41598-019-41851-5
74. Ji X, Liu J (2015) Associations between Blood Zinc Concentrations and Sleep Quality in Childhood: A Cohort Study. Nutrients 7 (7):5684-5696. doi:10.3390/nu7075247
75. Lee YF, Gerashchenko D, Timofeev I, Bacskai BJ, Kastanenka KV (2020) Slow Wave Sleep Is a Promising Intervention Target for Alzheimer's Disease. Front Neurosci 14:705.

doi:10.3389/fnins.2020.00705

76. Lucey BP, McCullough A, Landsness EC, Toedebusch CD, McLeland JS, Zaza AM, Fagan AM, McCue L, Xiong C, Morris JC, Benzinger TLS, Holtzman DM (2019) Reduced non-rapid eye movement sleep is associated with tau pathology in early Alzheimer's disease. Sci Transl Med 11 (474). doi:10.1126/scitranslmed.aau6550

# Figures

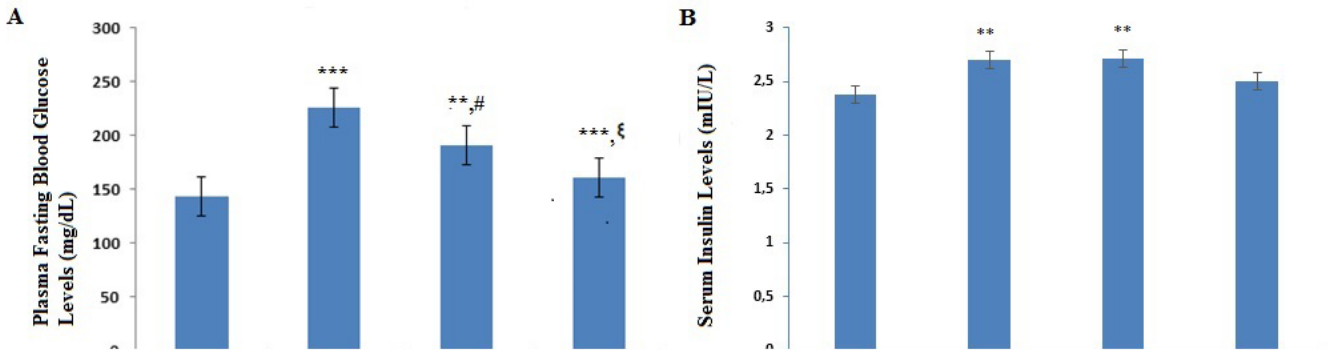


## Figure 1

A: Plasma fasting blood glucose in SH and experimental groups, n=6; B: Serum insülin levels in SH and experimental groups, n=8; C: Hippocampus insülin levels in SH and experimental groups, n=6; D: HOMA-IR levels, n=6; E: Total brain AβO levels in SH and experimental groups, n=8; F: Hippocampus AβO levels in

SH and experimental groups, n=8. Results are presented as mean ±SEM. (*: Significant vs SH group, #: Significant vs SHZ group, ξ: Significant vs AD group. *: p<0.05; **: p<0.01; ***: p<0.001, #: p<0.05; ##: p<0.01; ###: p<0.001, ξ: p<0.05, ξξ: p<0.01, ξξξ: p<0.001)

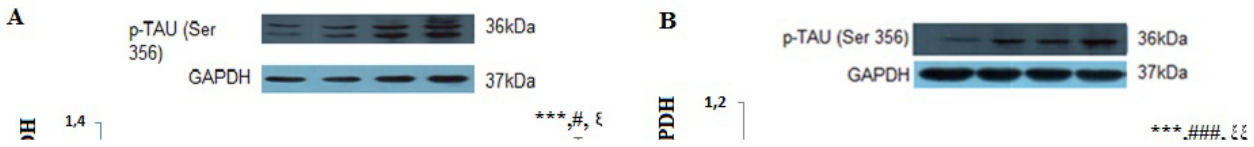


**Figure 2**

A: Total brain p-Tau (Ser356) levels in SH and experimental groups, n=6; B: Hippocampus p-Tau (Ser356) levels in SH and experimental groups, n=6; C: Total brain p-IRS1 (Ser612) levels in SH and experimental groups, n=6; D: Hippocampus p-IRS1 (Ser612) levels in SH and experimental groups, n=7. E: Total brain p-GSK3β (Ser21) levels in SH and experimental groups, n=7; F: Hippocampus p-GSK3β (Ser21) levels in SH and experimental groups, n=8. Results are presented as mean ±SEM. (*: Significant vs SH group, #: Significant vs SHZ group, ξ: Significant vs AD group. *: p<0.05; **: p<0.01; ***: p<0.001, #: p<0.05; ##: p<0.01; ###: p<0.001, ξ: p<0.05, ξξ: p<0.01, ξξξ: p<0.001)

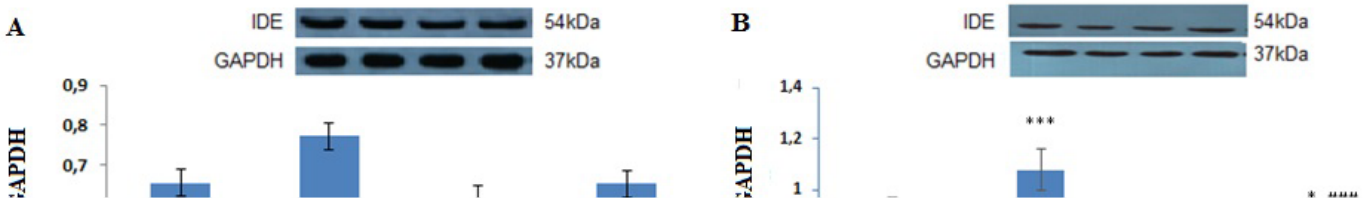


## Figure 3

A: Total brain IDE levels in SH and experimental groups, n=6; B: Hippocampus IDE levels in SH and experimental groups, n=6; C: Total brain NEP levels in SH and experimental groups, n=7; D: Hippocampus NEP levels in SH and experimental groups, n=6. Results are presented as mean ±SEM. (*: Significant vs SH group, #: Significant vs SHZ group, ξ: Significant vs AD group. *: p<0.05; **: p<0.01; ***: p<0.001, #: p<0.05; ##: p<0.01; ###: p<0.001, ξ: p<0.05, ξξ: p<0.01, ξξξ: p<0.001)

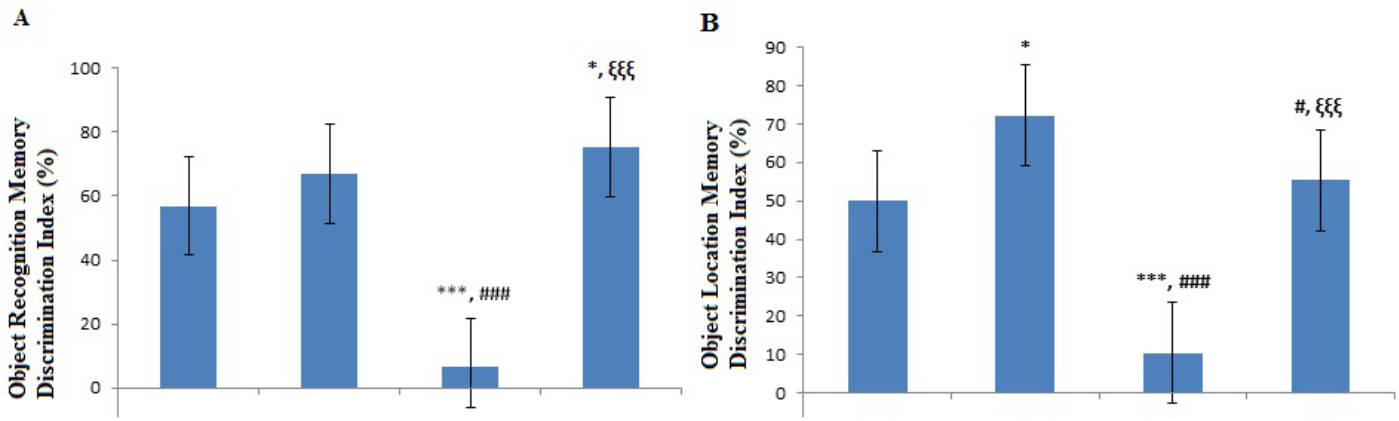


## Figure 4

A: The object recognition memory discrimination index in SH and experimental groups, n=11; B: The object location memory discrimination index in SH and experimental groups, n=10. Results are presented as mean ±SEM. (*: Significant vs SH group, #: Significant vs SHZ group, ξ: Significant vs AD group. *: p<0.05; **: p<0.01; ***: p<0.001, #: p<0.05; ##: p<0.01; ###: p<0.001, ξ: p<0.05, ξξ: p<0.01, ξξξ: p<0.001)

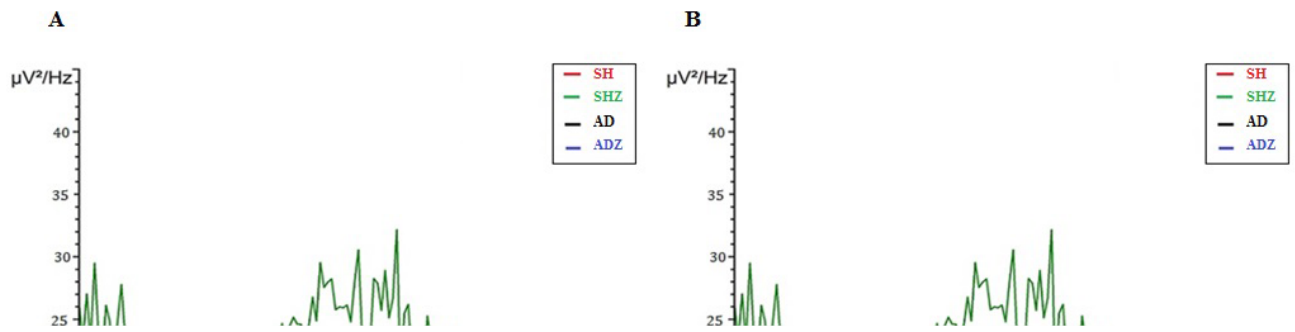


## Figure 5

A: Power spectrum changes in the delta frequency band recorded from the left temporal (T3) electrode region in SH and experimental groups; B: Power spectrum changes in the spindle frequency band recorded from the left temporal (T3) electrode region in SH and experimental groups; C: The correlations between object recognition memory discrimination index and left temporal (T3) spindle power spectra; D: The correlations between object location memory discrimination index and left temporal (T3) spindle power spectra.